Rac1 Is a Novel Regulator of Contraction-Stimulated Glucose Uptake in Skeletal Muscle

Lykke Sylow,[1] Thomas E. Jensen,[1] Maximilian Kleinert,[1] Joshua R. Mouatt,[1] Stine J. Maarbjerg,[4] Jacob Jeppesen,[1] Clara Prats,[5] Tim T. Chiu,[2] Shlomit Boguslavsky,[2] Amira Klip,[2] Peter Schjerling,[3] and Erik A. Richter[1]

In skeletal muscle, the actin cytoskeleton-regulating GTPase, Rac1, is necessary for insulin-dependent GLUT4 translocation. Muscle contraction increases glucose transport and represents an alternative signaling pathway to insulin. Whether Rac1 is activated by muscle contraction and regulates contraction-induced glucose uptake is unknown. Therefore, we studied the effects of in vivo exercise and ex vivo muscle contractions on Rac1 signaling and its regulatory role in glucose uptake in mice and humans. Muscle Rac1-GTP binding was increased after exercise in mice (~60–100%) and humans (~40%), and this activation was AMP-activated protein kinase independent. Rac1 inhibition reduced contraction-stimulated glucose uptake in mouse muscle by 55% in soleus and by 20–58% in extensor digitorum longus (EDL; $P < 0.01$). In agreement, the contraction-stimulated increment in glucose uptake was decreased by 27% ($P = 0.1$) and 40% ($P < 0.05$) in soleus and EDL muscles, respectively, of muscle-specific inducible Rac1 knockout mice. Furthermore, depolymerization of the actin cytoskeleton decreased contraction-stimulated glucose uptake by 100% and 62% ($P < 0.01$) in soleus and EDL muscles, respectively. These are the first data to show that Rac1 is activated during muscle contraction in murine and human skeletal muscle and suggest that Rac1 and possibly the actin cytoskeleton are novel regulators of contraction-stimulated glucose uptake. ***Diabetes*** **62:1139–1151, 2013**

Muscle contraction, like insulin, increases glucose uptake into skeletal muscle (1,2). Insulin and muscle contraction both stimulate the translocation of vesicles containing the glucose transporter GLUT4 from intracellular compartments to the sarcolemma and T tubules, allowing glucose to enter the cell via facilitated diffusion (3–5). However, the proximal signaling pathways of contraction and insulin are distinct. Muscle contraction has no effect on the insulin-signaling pathway (6,7), and muscle-specific knockout of the insulin receptor (8), or inhibition of phosphatidyl inositol 3-kinase with wortmannin (9) does not impair contraction-stimulated glucose uptake. Exercise has an insulin-sensitizing effect, suggesting that these two pathways may regulate similar unidentified distal signaling steps (10,11).

Activation of AMP-activated protein kinase (AMPK) and calcium-dependent signaling, such as protein kinase Cs (PKCs) and calcium-calmodulin–dependent kinases, has traditionally been believed to induce glucose uptake during muscle contraction (3,12). However, the functional significance of these pathways is not fully understood. It is likely that so far unrecognized mechanisms regulated by AMPK, PKCs, calcium, liver kinase B1, stretch, reactive oxygen, and nitrogen species, or other yet unidentified pathways, participate in the regulation of glucose uptake during muscle contraction (3,13).

One such candidate is Rac1 (Ras-related C3 botulinum toxin substrate 1), a small Rho family GTPase that regulates various cellular processes, including dynamic assembly and disassembly of the actin cytoskeleton (14,15). Rac1 is activated by insulin and induces actin cytoskeleton remodeling at the plasma membrane (15,16). Rac1-dependent rearrangement of the actin cytoskeleton is necessary for insulin-stimulated GLUT4 translocation in L6 myotubes (16–18).

Even though Rac1 has traditionally only been implicated in insulin signaling, the contraction-related protein, AMPK, has been proposed to activate Rac1 in cultured muscle cells (19), endothelial cells (20), and macrophages (21). The primary aim of the present investigation was to explore whether insulin-independent stimuli, such as exercise in vivo and muscle contractions in vitro, activate Rac1 in skeletal muscle. Because Rac1 activation is necessary for insulin-stimulated GLUT4 translocation (22), we further aimed to investigate the involvement of Rac1 in AICAR- and contraction-stimulated glucose uptake. We hypothesized that Rac1 is activated by muscle contraction and that this activation plays a role in contraction-induced glucose uptake.

RESEARCH DESIGN AND METHODS

Female C57BL/6 mice (Taconic, Denmark) aged 12–16 weeks were used for all inhibitor incubation experiments.

Muscle-specific kinase-dead α2-AMPK mice. Mice overexpressing a kinase-dead $Lys^{45}Arg$ mutant α_2-AMPK subunit, driven by the heart- and skeletal muscle–specific creatine kinase promoter (AMPK α2-KD), have been described previously (23). The male transgenic AMPK α2-KD and wild-type (WT) mice (12–16 weeks old) used were littermates from intercross-breeding of hemizygous transgenic mice and WT mice.

Tetracycline-inducible muscle-specific Rac1 knockout mice. Rac1 floxed mice (24) were crossed with mice containing a tetracycline-controlled transactivator coupled to the human skeletal actin promoter, which drives the muscle specific expression of the Cre recombinase (25). Mice were backcrossed until N5 (96.9% congenic) on a C57BL/6 background. Male transgenic

From the [1]Molecular Physiology Group, Department of Nutrition, Exercise and Sports, University of Copenhagen, Copenhagen, Denmark; the [2]Program in Cell Biology, The Hospital for Sick Children, Toronto, Ontario, Canada; the [3]Institute of Sports Medicine, Department of Orthopedic Surgery, Bispebjerg Hospital and Center for Healthy Aging, Faculty of Health Sciences, University of Copenhagen, Copenhagen, Denmark; [4]Clinical Pharmacology Diabetes, Novo Nordisk A/S, Søborg, Denmark; and the [5]Department of Biomedical Sciences, Center for Healthy Aging, University of Copenhagen, Copenhagen, Denmark.

Corresponding author: Erik A. Richter, erichter@ifi.ku.dk.

Received 19 April 2012 and accepted 7 November 2012.

DOI: 10.2337/db12-0491

This article contains Supplementary Data online at http://diabetes.diabetesjournals.org/lookup/suppl/doi:10.2337/db12-0491/-/DC1.

See accompanying commentary, p. 1024.

mice (14–18 weeks old) were littermates from breeding of heterozygous Cre and Rac1 fl/fl transgenic mice. Rac1 knockout (KO) was obtained by adding the tetracycline analog doxycycline (1 g/L; Sigma-Aldrich) to the drinking water for 21 days, after which it was switched to normal tap water (doxycycline treatment was initiated at age 5–7 weeks). Mice were used for experiments after receiving tap water for 4–6 weeks. Control WT mice were given tap water.

All animals were maintained on a 10:14-h light/dark cycle and received a standard rodent chow diet (Altromin No. 1324; Chr. Pedersen, Ringsted, Denmark) and water ad libitum. All experiments were approved by the Danish Animal Experimental Inspectorate and complied with the "European Convention for the Protection of Vertebrate Animals Used for Experiments and Other Scientific Purposes."

Muscle incubation. Soleus and extensor digitorum longus (EDL) muscles were dissected from 2-h fasted, anesthetized mice (6 mg pentobarbital sodium/100 g body wt) and suspended at resting tension (4–5 mN) in incubation chambers (Multi Myograph System; Danish Myo-Technology, Denmark) in Krebs-Ringer-Henseleit (KRH) buffer supplemented with 0.1% BSA, 2 mmol/L pyruvate, and 8 mmol/L mannitol at 30°C, as described previously (26). For inhibitor experiments, the muscles were preincubated for 50 min in KRH buffer with the Rac1 inhibitors, NSC23766 (200 μmol/L; Calbiochem) or Rac1 Inhibitor II (10 μmol/L; Calbiochem), or Latrunculin B (10 and 1 μmol/L; Sigma-Aldrich), or a corresponding amount of DMSO as the vehicle control. Contractions were induced by electrical stimulation every 15 s with 2-s trains of 0.2-ms pulses delivered at 100 Hz (~35 V) for 10 min. For AICAR experiments, muscles were preincubated for 20 min, followed by 40 min of AICAR stimulation (2 mmol/L). Passive stretch was obtained by manually stretching soleus muscle at a tension of 150 mN for 15 min.

2-Deoxyglucose uptake. 2-Deoxyglucose (2DG) uptake was measured for 10 min during the electrical stimulation using ^{3}H and ^{14}C radioactive tracers, as described previously (26).

Mouse treadmill-running protocol. All animals were acclimatized to the treadmill three times before the experimentation day and tested for their maximal running capacity. On the experimental day, fed WT mice were exercised at 50 or 70% of their maximal running speed at 0% incline (16 m/min and 22.3 m/min, respectively). For the AMPK α2-KD study, AMPK α2-KD or WT control mice were exercised at 70% (WT: 22.7 m/min, AMPK α2-KD: 16 m/min) of their maximal running speed (27). Nonexercised resting mice were placed on the treadmill apparatus while it was turned off. Immediately after the exercise bout, mice were killed by cervical dislocation and quadriceps muscles were quickly removed and stored at −80°C until further processing.

Subcellular fractionation of mouse muscle. To separate surface membrane from other compartments, we used a subcellular fractionation technique of fresh mouse hind limb (gastrocnemius and quadriceps) muscles in the basal state, as previously described (28,29). This technique allows distinction of plasma membranes (P1 and P2) from the cytosol and low-density intracellular membranes (F1-F8).

Cell culture. C2C12-GLUT4myc myoblasts (30) were maintained in an atmosphere of 5% CO_2 at 37°C with Dulbecco's modified Eagle's medium containing 4.5 g/L glucose and 10% FBS (v/v), 5 mg/mL Blasticidin–HCl, and antibiotics. C2C12-GLUT4myc myoblasts were differentiated into myotubes, as previously described (30), and serum-starved for 3 h before stimulations with insulin (100 nmol/L, 10 min), 2,4 Dinitrophenol (0.5 mmol/L, 20 min; DNP), or AICAR (2 mmol/L, 30 min). Rac1 GTP binding was measured, as described earlier, for L6 myotubes (16). Briefly, immediately after treatments, cells were placed on ice, washed twice with ice-cold PBS, and lysed in 400 μL buffer containing 150 mmol/L NaCl, 10 mmol/L $MgCl_2$, 5 mmol/L HEPES (pH 7.5), 2% glycerol, 1% Igepal, 1 mmol/L $NaVO_4$, 1 mmol/L EDTA, 20 μL/mL protease inhibitor cocktail (BD Biosciences, Canada), and 1 mmol/L phenylmethylsulfonyl fluoride. Lysates (300 μL) were loaded onto Sepharose beads with conjugated p21-binding domain (PBD) of p21 activated kinase (PAK) to pull down activated Rac, which was visualized by SDS-PAGE and immunoblotting. GLUT4 translocation was measured as previously described (30).

Human experiments. All potential subjects were given oral and printed information on the study design and its risks and gave written, informed consent. The study was approved by the Copenhagen Ethics Committee (Reg. No. HKF277313) and conducted in accordance with the Declaration of Helsinki II (1996). Healthy, young, normal-weight [26 ± 2 years, 85 ± 2 kg, 184 ± 2 cm, peak V_{O_2} ($V_{O_{2peak}}$) = 58 ± 2 mL O_2 · kg body weight^{-1} · min^{-1}] men volunteered to participate. After an overnight fast, muscle biopsy specimens were taken under local anesthesia from the soleus and gastrocnemius muscles with a Bergstrom 5-mm needle with applied suction before and immediately after 45 min of 15% inclined treadmill walking at a speed of 6.3 ± 0.1 km/h and 69.1 ± 1.6% $V_{O_{2\ peak}}$. Muscle fiber type composition and activation of several kinases in muscle during exercise in these subjects has been reported elsewhere (31).

Muscle analyses. Immediately after electrical stimulation or exercise, mouse and human muscle tissue was quickly frozen in liquid nitrogen and stored at –80°C. Tissue was homogenized 2 × 1 min at 30 Hz using a Tissuelyser II (Qiagen, U.S.) in ice-cold Rac1 buffer (Rac1-buffer was used for the Rac1-activity assay and are commercially available from Cytoskeleton Inc.) or in 50 mmol/L HEPES (pH 7.5), 150 mmol/L NaCl, 20 mmol/L sodium pyrophosphate, 20 mmol/L β-glycerophosphate, 10 mmol/L NaF, 2 mmol/L sodium orthovanadate, 2 mmol/L EDTA, 1% NP-40, 10% glycerol, 2 mmol/L phenylmethylsulfonyl fluoride, 1 mmol/L $MgCl_2$, 1 mmol/L $CaCl_2$, 10 μg/mL leupeptin, 10 μg/mL aprotinin, and 3 mmol/L benzamidine. After rotation end-over-end for 1 h, lysate supernatants were collected by centrifugation (13,000*g*) for 20 min at 4°C.

Immunoblotting. Lysate protein concentrations were analyzed using the bicinchoninic acid method using BSA standards (Pierce) and bicinchoninic acid assay reagents (Pierce). Total protein and phosphorylation levels of relevant proteins were determined by standard immunoblotting techniques loading equal amounts of protein. The primary antibodies used were p-AMPK Thr^{172}, p-ACC^{Ser212}, PAK1, actin, GLUT4, p-Rac1/$Cdc42^{Ser71}$, p-Akt substrate (PAS), p-PAK^{Thr423}, p-$TBC1D1^{Ser237}$, p-$TBC1D4^{Thr642}$ (Cell Signaling Technology), anti-VAMP3 (Synaptic Systems), and Rac1 (Millipore). Polyvinylidene difluoride membranes (Immobilon Transfer Membrane, Millipore) were blocked in TBS-Tween 20 containing 2% skim milk protein for 30 min at room temperature. Membranes were incubated with primary antibodies overnight at 4°C, followed by incubation with horseradish peroxidase-conjugated secondary antibody for 1 h at room temperature. Bands were visualized using an Eastman Kodak Image Station 2000MM and enhanced chemiluminescence (ECL^{+}; Amersham Biosciences).

Rac1 activation assay in muscle samples. Frozen solei, EDL, gastrocnemius, and quadriceps muscles were pulverized and homogenized at 30 Hz for 1 min using a Tissuelyser II (Qiagen, U.S.). Lysates were generated by centrifuging the homogenate for 2 min at 10,000*g*. Rac1 activities were measured in the supernatant using a commercially available Rac1 activation assay kit (BK 126, Cytoskeleton Inc.). In short, lysates were loaded onto wells coated with the PBD domain of PAK. This domain specifically only binds Rac1 in its GTP-bound form. GTP-bound Rac1 was thus bound to the PBD-coated wells and the amount of GTP-bound Rac1 was detected using a colorimetric assay.

Immunohistochemistry on single muscle fibers. Basal or exercised EDL muscles were immersed in cold Krebs-Henseleit bicarbonate buffer containing procaine hydrochloride (35 mg/10 mL) for 5 min and then fixed with 2% formaldehyde supplemented with 0.15% picric acid during 30 min at room temperature after 3.5 h at 4°C. After isolation of a minimum of 30 single muscle fibers per muscle, immunostaining against Rac1 was performed, as previously described (32). Briefly, isolated muscle fibers were incubated overnight with a dilution of the anti-Rac1 (Novus Biologicals) in immunobuffer, and after three washes of 20 min each with immunobuffer, the primary antibody was immunodetected by binding of a secondary conjugated with Alexa Fluor 568 or 488 (Invitrogen, U.K.). Negative controls for each of the staining conditions were performed by staining without primary antibody. Muscle fibers were mounted in Vectashield mounting medium and analyzed. Confocal images were acquired with a Zeiss LSM710 microscope through a 63 × /1.40 oil DIC Plan-Apochromatic objective at 20°C. Images were analyzed using ZEN (2011) software.

Statistical analyses. Results are presented as mean ± SEM. Statistical testing was performed using paired *t* tests or one- or two-way repeated-measures ANOVA as appropriate. The Tukey post hoc test was used when appropriate. Statistical evaluation was performed using SigmaPlot 11.0 software. The significance level was set at $P < 0.05$.

RESULTS

Rac1 expression is higher in oxidative muscle and is localized to plasma membranes. In mice, Rac1 protein was 40–50% more abundant in the oxidative soleus than the more glycolytic EDL and mixed gastrocnemius muscles (Fig. 1*A*). Expression of Rac1 also tended to be 30% higher ($P = 0.06$) in gastrocnemius compared with EDL muscle. In humans, the Rac1 expression pattern was similar between soleus and gastrocnemius (Fig. 1*B*). This agrees with a more homogeneous fiber-type composition in human muscles, as previously demonstrated in these subjects (31). Subcellular fractionations showed that Rac1 was mainly localized to plasma membranes (P1 and P2) in mouse hind limb muscles (Fig. 1*C*), consistent with previous findings in other cell types (33,34). The control

protein, VAMP3, was localized primarily to intracellular fractionations (Fig. 1*C*), as previously published (35).

Rac1 is activated by electrically induced contraction, passive stretching, and after 30 min of treadmill running in mouse muscle. Rac1 is activated when bound to GTP (15). We therefore investigated if Rac1-GTP binding was increased in response to electrically induced contraction, stretch, and treadmill running in mouse skeletal muscle. Rac1-GTP binding was 61% higher after electrically induced contraction (Fig. 2*A*) and 50% higher after passive stretching (Fig. 2*B*) in incubated mouse soleus muscles (in which Rac1 is most abundant). Furthermore, Rac1-GTP binding was increased by 44% after 30 min of treadmill running at a relative low running speed of 40% maximum running speed (10 m/min; Fig. 2*C*). We also assessed whether Rac1-GTP binding and phosphorylation of the Rac1 downstream target, PAK1 (p-PAK1^{Thr423}), both increased in an intensity-dependent manner during exercise in mice. Rac1-GTP binding increased by ~50% and 100% after treadmill running at 50% and 70% of maximum running speed, respectively. p-PAK^{Thr423} mimicked Rac1-GTP binding and was increased by ~60% and 100% at these intensities. Rac1 has previously been found to relocalize when bound to GTP. We therefore isolated single fibers from basal or exercised EDL muscles and visualized Rac1 localization at the cell periphery using confocal fluorescence immunohistochemistry. In the basal state, Rac1 presented a striated pattern. After exercise, this structure thickened by ~100% measured by determining the full width at half maximum (FWHM; Fig. 2*E*).

Rac1 activity is increased after exercise in humans. To ascertain whether Rac1 activation also occurs in human muscle, Rac1-GTP binding and serine 71 phosphorylation of Rac1 (p-Rac1^{Ser71}), which correlates with Rac1-GTP

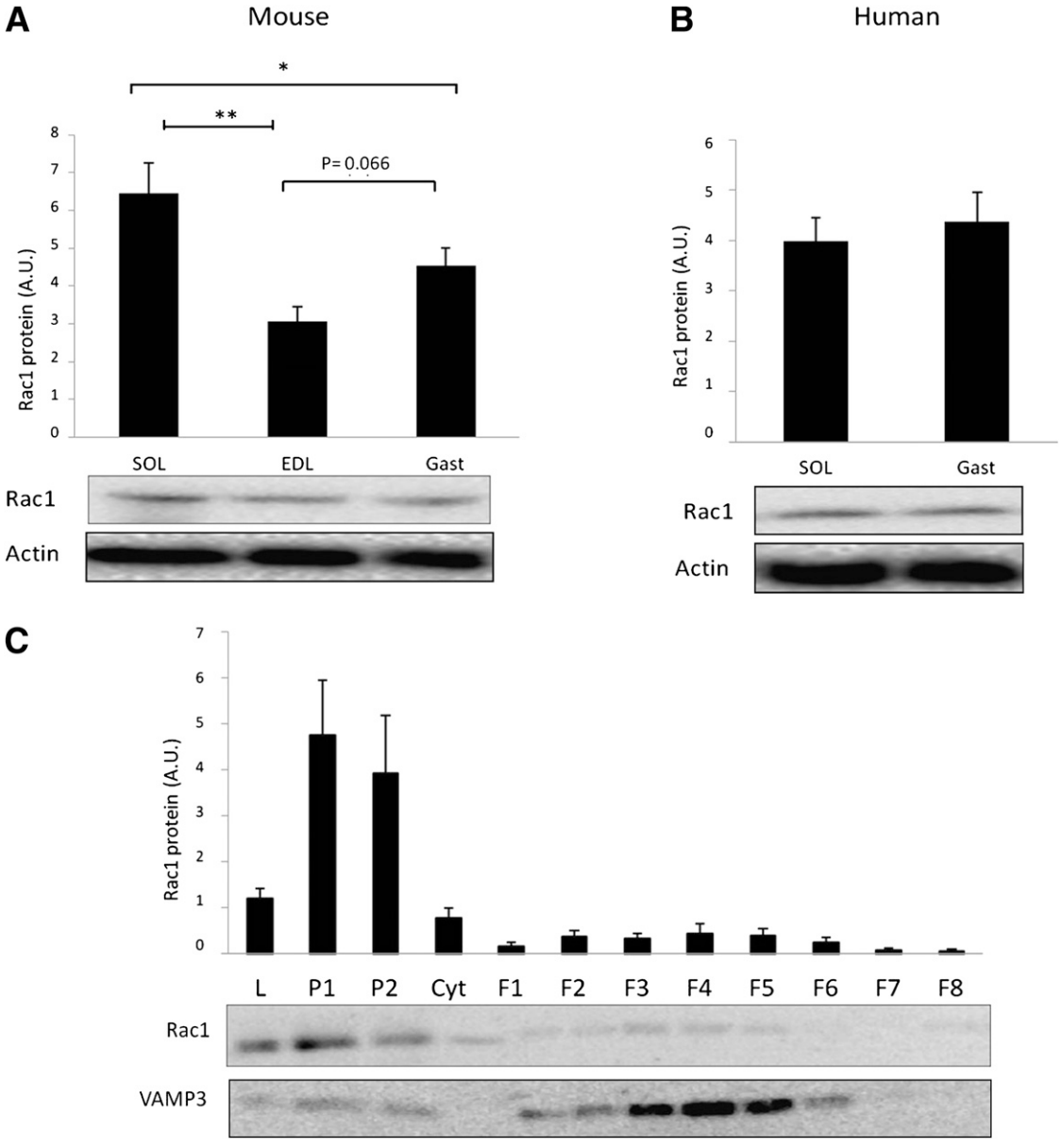

FIG. 1. ***A*: Rac1 protein expression in mouse soleus (SOL), extensor digitorum longus (EDL), and gastrocnemius (Gast) (n = 9).** ***B*: Rac1 expression in human soleus and gastrocnemius (n = 8).** ***C*: Intracellular localization of Rac1 and VAMP3 in mouse hind limb (gastrocnemius and quadriceps) muscle. L, lysate; P1 and 2, plasma membrane fractions; Cyt, cytosol; F1-8 intracellular fractions (n = 7). Statistical significance is indicated by *P < 0.05; ** P < 0.01. Values represent mean ± SEM.**

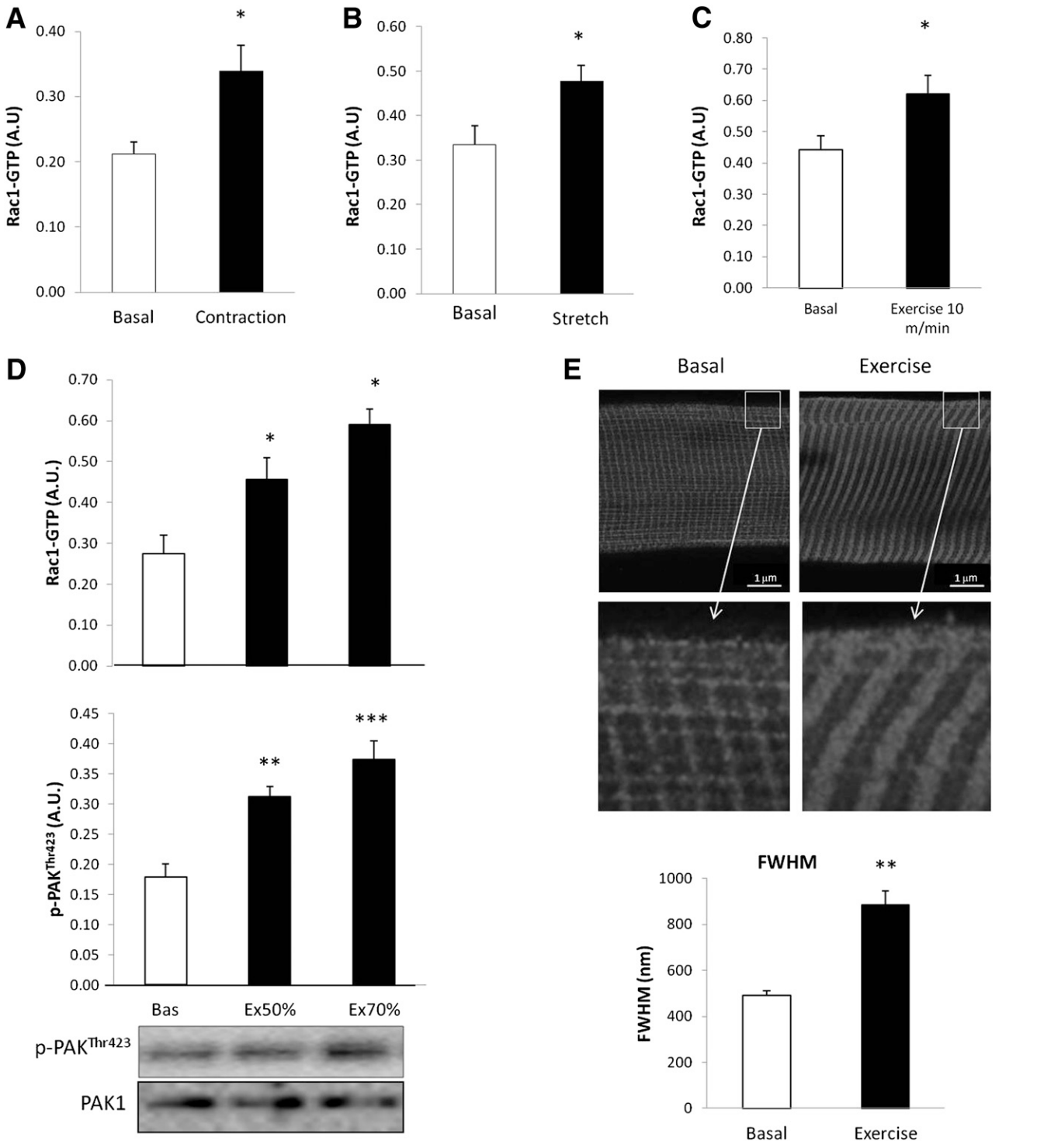

FIG. 2. *A*: **Rac1-GTP binding in incubated mouse soleus muscle stimulated with (black bar) or without (white bar) electrically induced contraction (100 Hz 15-s intervals, 2-s train, 0.2-ms impulses) (n = 7).** *B*: **Rac1-GTP binding in incubated mouse soleus muscle kept at resting tension (2–5 mN; basal) or stretched (150 mN, 15 min) (n = 7).** *C*: **Mouse quadriceps muscle, basal and after 30 min running at speed of 10 m/min (exercise 10 m/min = 40% of max running speed) (n = 7).** *D*: **Rac1-GTP binding (*top*) and p-PAK^{Thr423} (*middle*), and representative blots (*bottom*) in mouse quadriceps muscle basal or in response to 30-min treadmill running at 50 or 70% (Ex 50/70%) of maximum running speed (n = 8).** *E*: **Representative images and bar graph (FWHM) showing Rac1 staining of single fibers isolated from mouse EDL muscle in the basal state or after 30 min of treadmill running at 70% of maximum running speed (n = 5). Statistical significance compared with basal is indicated by *P < 0.05; **P < 0.01; ***P < 0.001. Values represent mean ± SEM.**

binding in CaCo-2 cells (36), were measured in soleus and gastrocnemius muscle of lean, healthy individuals before and immediately after 45 min of inclined walking at ~69.1% $V\text{O}_{2\text{peak}}$. Rac1-GTP binding was elevated by 52% in soleus and 38% in gastrocnemius (Fig. 3*A* and *B*), and p-Rac1^{Ser71} increased 39% in soleus and 20% in gastrocnemius, but the increase in gastrocnemius was not significant (Fig. 3*C*). In addition, p-PAK1^{Thr423} increased after

exercise by 102% in soleus and 83% in gastrocnemius muscles (Fig. 3*D*).

Rac1 is not activated downstream of AMPK, and exercise-stimulated Rac1 activation is AMPK independent. AMPK is activated during muscle contraction, and AMPK activation by AICAR and retinoic acid has previously been reported to activate Rac1 in vitro in C2C12 myotubes (19). In the current study, however, AICAR failed to activate Rac1 in mouse soleus and EDL muscles despite a significant increase in p-AMPK^{Thr172} and p-ACC^{Ser212} (Fig. 4*A* and *B*). In C2C12 myotubes, only insulin increased Rac1-GTP binding. Neither DNP (a mitochondrial uncoupler) nor AICAR changed Rac1-GTP binding, despite significant increases in p-AMPK^{Thr172} and p-ACC^{Ser212} (Fig. 4*C*). It is possible, however, that AMPK activation is necessary for contraction-induced activation of Rac1. Therefore, Rac1-GTP binding in quadriceps of WT and AMPK α2-KD mice was compared after treadmill running. We previously showed severely compromised AMPK signaling during exercise in AMPK α2-KD compared with WT mice (27). Treadmill running at 70% of maximal running speed significantly increased Rac1-GTP binding (Fig. 4*D*) by ~100% in WT and AMPK α2-KD mice. These data suggest that AMPK activation is neither sufficient nor necessary to activate Rac1 in intact skeletal muscle or muscle cells in culture.

Pharmacological inhibition of Rac1 decreases contraction-stimulated 2DG uptake. To test whether Rac1 is necessary for contraction-induced glucose uptake, mouse soleus and EDL muscles were isolated and incubated with or without the Rac1 inhibitors NSC23766 and Rac1 inhibitor II. The concentrations used were the lowest necessary to inhibit insulin-stimulated Rac1 activation, as found in pilot experiments (data not shown). Contraction-stimulated glucose uptake was decreased by NSC23766 by ~55% in soleus and EDL muscles (Fig. 5*A*). Similarly, Rac1 inhibitor II inhibited the contraction-stimulated increment in glucose uptake in soleus and EDL by 58% and 22%, respectively (Fig. 5*B*). None of the inhibitors affected p-AMPK^{Thr172} or p-ACC^{Ser212} signaling (Fig. 5*C* and *D*), initial force production, or fatigue development (Supplementary Fig. 1*A*). In EDL muscle, contraction increased

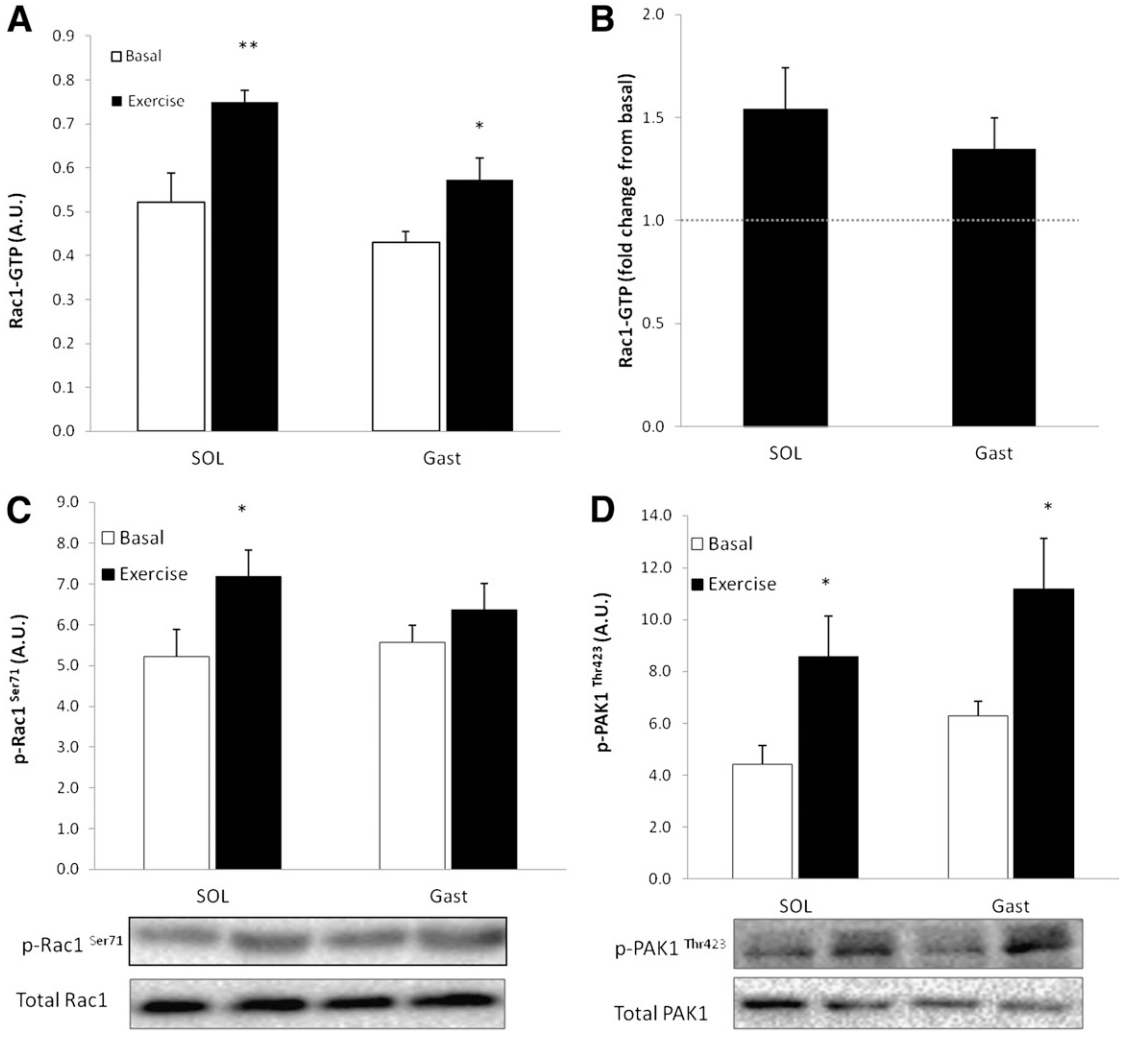

FIG. 3. ***A*****: Rac1-GTP binding in human soleus (SOL) and gastrocnemius (Gast) in the basal state and after 45 min of inclined walking at ~69% $V_{O_2\ peak}$ (*n* = 5–9).** ***B*****: Exercise-stimulated fold changes from basal in soleus (SOL) and gastrocnemius (Gast).** ***C*****: Bar graph and representative Western blot analysis of p-Rac1^{Ser71} in response to exercise in human soleus and gastrocnemius muscle (*n* = 5–9).** ***D*****: Bar graph and Western blot analysis of p-PAK^{Thr423} in response to exercise in human soleus and gastrocnemius muscle (*n* = 5–9). Statistical significance compared with basal is indicated by **P* < 0.05; ***P* < 0.01. Values represent mean ± SEM.**

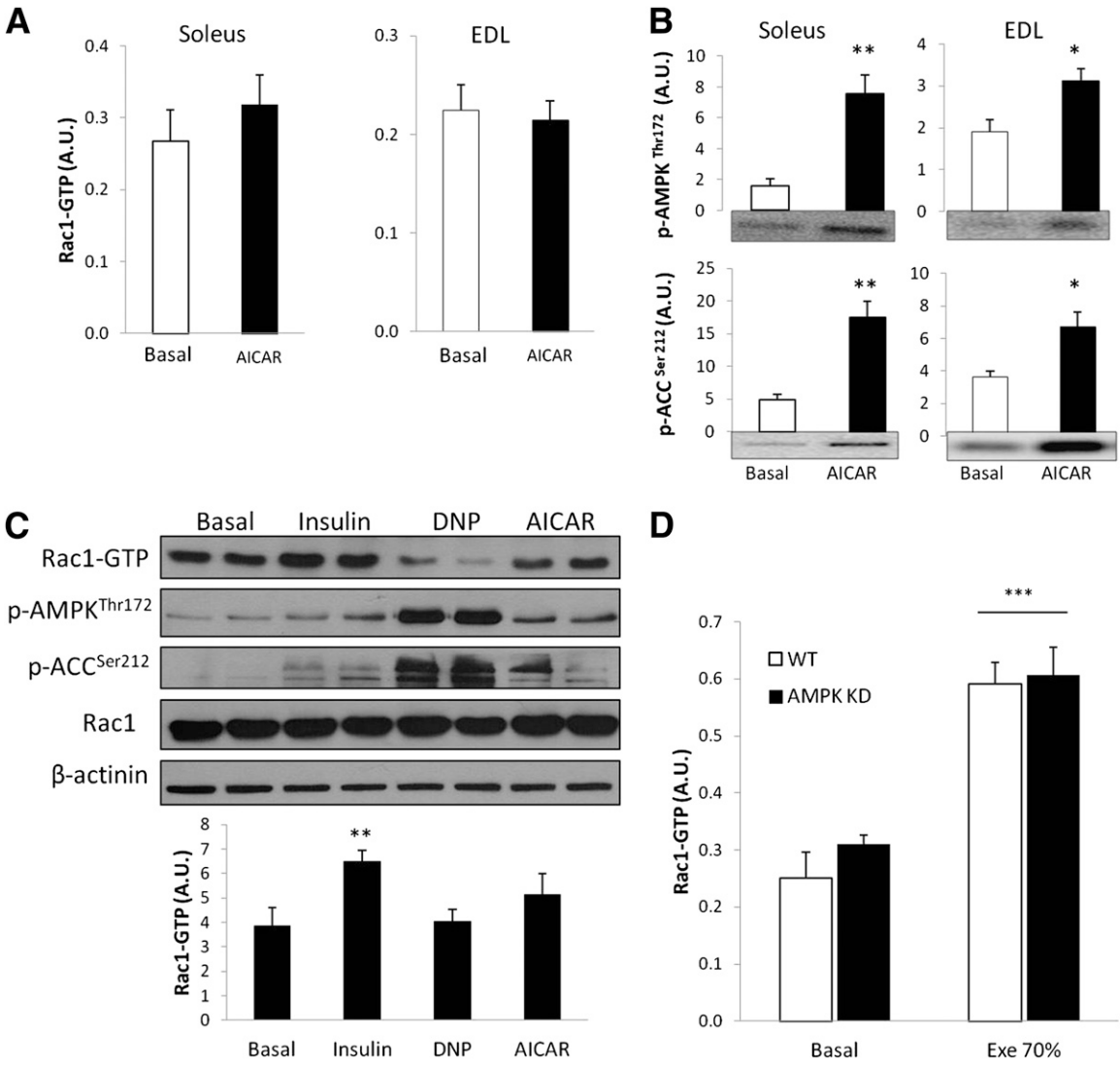

FIG. 4. ***A*: Rac1-GTP binding after ex vivo AICAR (2 mmol/L) stimulation of mouse soleus and EDL muscles (n = 5–6). *B*: Bar graphs and representative blots showing p-AMPK^{Thr172} and p-ACC^{Ser212} in response to AICAR (n = 5–6). *C*: Representative blots and bar graphs of the effect of insulin (100 nmol/L; 10 min), DNP (0.5 mmol/L; 20 min), and AICAR (2 mmol/L; 30 min) on Rac1-GTP binding in C2C12 myotubes (n = 5). *D*: Rac1-GTP binding in WT and AMPK KD mouse quadriceps muscle basal or in response to 30 min of treadmill running at 70% (Exe 70%) of the maximum running speed (n = 6–9). Statistical significance compared with basal is indicated by *$P < 0.05$; **$P < 0.01$; ***$P < 0.001$. Values represent mean ± SEM.**

p-PAK1^{Thr423} by ~42%, and this response was blunted by Rac1 Inhibitor II (Fig. 5*D*). There was no increase in p-PAK1^{Thr423} in soleus in response to electrically induced contraction, but the Rac1 Inhibitor II decreased p-PAK1^{Thr423} (Fig. 5*D*). No effects of the inhibitors were observed on Rac1 or GLUT4 protein expression (Fig. 5*C* and *D*). Rac1 Inhibitor II did not affect the 83% increase in insulin-stimulated glucose uptake in white adipose (gonadal) tissue (Fig. 5*E*).

Contraction-stimulated 2DG uptake is depressed in muscle-specific inducible Rac1 KO mice. Rac1 protein content was reduced 65% in soleus and 90% in EDL from doxycycline-treated inducible muscle-specific Rac1 KO mice compared with WT control mice (Fig. 6*A*). Initial experiments showed that carrying the flox sequence, without activating the Cre-recombinase with doxycycline, did not affect Rac1 expression in muscle compared with WT mice. Furthermore, doxycycline treatment of WT mice did not affect Rac1 expression (Fig. 6*B*). After doxycycline treatment, the contraction-stimulated increment in 2DG uptake tended to be decreased by 27% ($P = 0.1$) in soleus and was significantly decreased by 40% ($P < 0.05$) in EDL muscle (Fig. 6*C* and *D*). No difference in GLUT4 content (Fig. 6*E* and *G*) or p-AMPK^{Thr172}, p-ACC^{Ser212}, p-TBC1D1^{Ser237}, TBC1D4^{Thr642}, or PAS signaling was observed between genotypes (Fig. 6*E* and *F*), and Rac1 KO did not affect force production (Supplementary Fig. 1*B*). Interestingly we observed that PAK1 protein expression was increased by ~20% in the Rac1 KO EDL muscle (Fig. 6*G*). When related to total protein, p-PAK1^{Thr423} was diminished in EDL in Rac1 KO mice compared with WT. When interpreted together with the results using Rac1 inhibitors, these data strongly implicate Rac1 in the regulation of contraction-stimulated glucose uptake in skeletal muscle.

Rac1 is not involved in AICAR-stimulated glucose uptake. Because Rac1-GTP binding did not increase in response to AICAR, we hypothesized that AICAR-stimulated glucose uptake would be normal in muscles

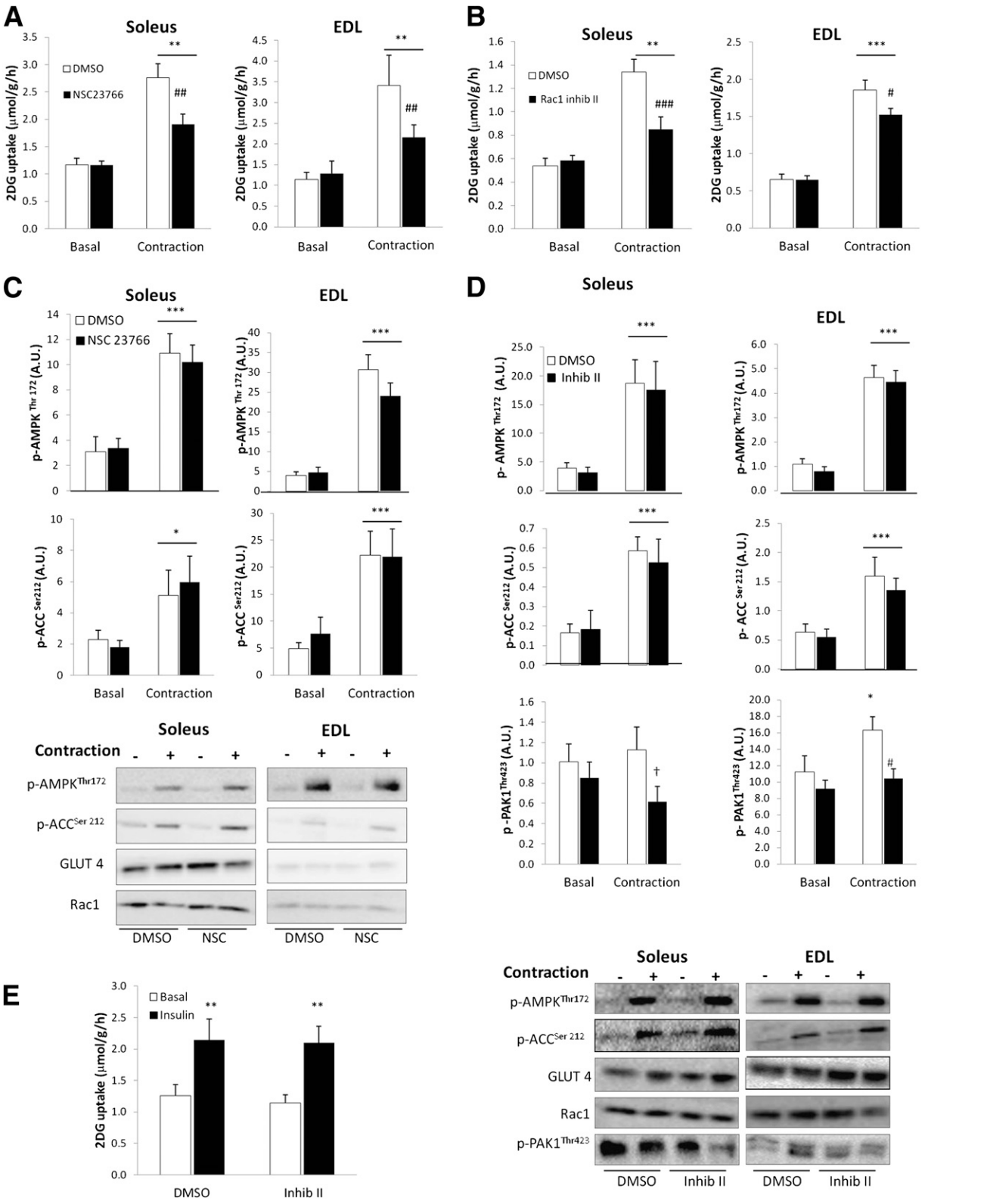

FIG. 5. *A*: Contraction-stimulated 2DG uptake in soleus and EDL without or with 200 μmol/L NSC23766, 1-h preincubation (n = 12). *B*: Contraction-stimulated 2DG uptake in soleus and EDL without or with 10 μmol/L Rac1 Inhibitor II (Inhib II), 1-h preincubation (n = 10). *C*: Representative blots and bar graphs show contraction-stimulated p-AMPK^{Thr172} and p-ACC^{Ser212} in soleus and EDL muscle without or with 200 μmol/L NSC23766. *D*: Representative blots and bar graphs show contraction-stimulated p-AMPK^{Thr172}, p-ACC^{Ser212}, and p-PAK^{Thr423} signaling and Rac1 and GLUT4 total protein in soleus and EDL muscle without or with 10 μmol/L Rac1 Inhibitor II (Inhib II). *E*: Insulin-stimulated (60 nmol/L) 2DG uptake in mouse white adipose (gonadal) tissue without or with 10 μmol/L Rac1 Inhibitor II (Inhib II), 1-h preincubation (n = 8). Statistical significance between basal and contraction is indicated by *P < 0.05; **P < 0.01; ***P < 0.001. Effect of inhibitor on contraction-stimulated 2DG or p-PAK^{Thr423} is indicated by #P < 0.05; ##P < 0.01; ###P < 0.001. Main effect of inhibitor is indicated by †P < 0.05. Values represent mean ± SEM.

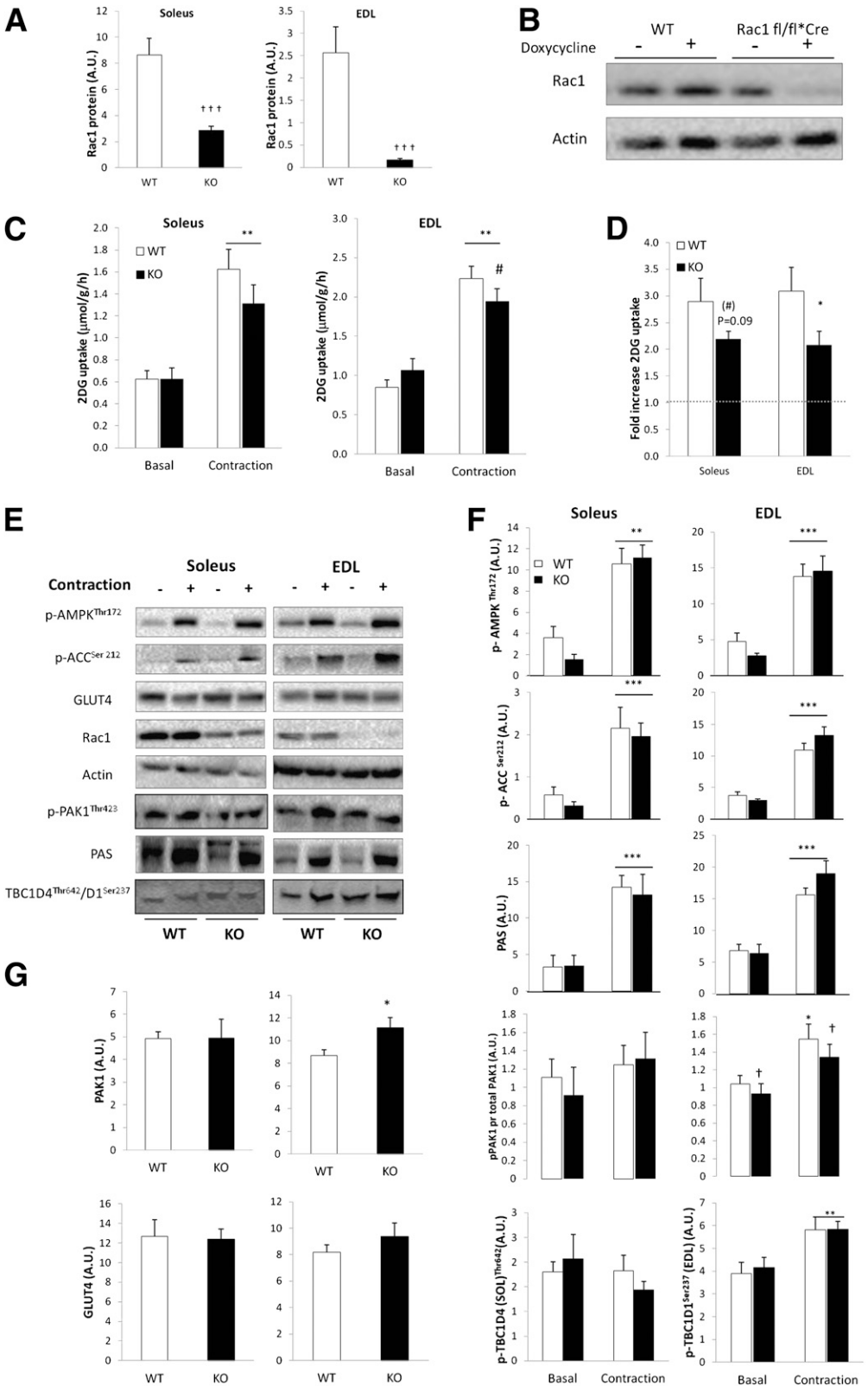

FIG. 6. ***A*: Bar graph shows mean ± SEM of Rac1 knockout efficiency in soleus and EDL muscle of muscle-specific inducible Rac1 KO mice and WT controls (n = 11–13). *B*: Representative Western blots showing the effect of doxycycline (1 g/L) treatment on Rac1 protein in WT vs. Floxed Rac1 KO mice (Rac1 fl/fl*Cre) (gastrocnemius muscle). *C*: Contraction-stimulated 2DG uptake in incubated isolated soleus and EDL muscles from WT and Rac1 KO mice (n = 11–13). *D*: Contraction-stimulated fold changes from basal in 2DG uptake in soleus and EDL from WT and Rac1 KO mice. *E*: Representative Western blots of p-AMPK^{Thr172}, p-ACC^{Ser212}, PAS, p-PAK^{Thr423}, p-TBC1D4^{Thr642} (Soleus), p-TBC1D1^{Ser237} (EDL), and actin, GLUT4, and Rac1 total proteins in response to contraction. *F*: Bar graph shows mean ± SEM of contraction-induced p-AMPK ^{Thr172}, p-ACC ^{Ser212}, PAS, p-PAK^{Thr423}/PAK1, p-TBC1D4^{Thr542}, and p-TBC1D1^{Ser237} in soleus and EDL from Rac1 KO mice and WT controls. *G*: Bar graph shows mean ± SEM of total PAK1 and GLUT4 protein in soleus and EDL of WT and Rac1 KO mice. Statistical significances between basal and contraction are indicated by *P < 0.05; **P < 0.01; ***P < 0.001. Effect of genotype on contraction-stimulated 2-DG and p-PAK^{Thr423} is indicated by #P < 0.05. Main effect of genotype is indicated by †P < 0.05; †††P < 0.001. Values represent mean ± SEM.**

preincubated with the Rac1 Inhibitor II and in Rac1 KO mice. In the inhibitor experiment, AICAR-induced a 30% and 100% increase in glucose transport in soleus and EDL, respectively (Fig. 7*A*). In agreement with our hypothesis, neither AICAR-induced glucose uptake nor signaling was affected by Rac1 Inhibitor II (Fig. 7*A*-*C*). These findings were confirmed in the Rac1 KO model, in which the ~40% and ~160% (SOL and EDL, respectively) AICAR-induced increment in 2DG uptake was unaffected by Rac1 KO (Fig. 7*D*). AMPK signaling was not affected by Rac1 KO (Fig. 7*E* and *F*). We did, however, observe that the Rac1 Inhibitor II (only in soleus), as well as Rac1 KO, induced a decrease in p-PAK^{Thr423} in response to AICAR (Fig. 7*B* and *E*). We also observed a 70% increase in PAK1 protein expression in EDL muscle in the Rac1 mice compared with WT (Fig. 7*E*).

To further confirm that Rac1 is not involved in AMPK-mediated glucose transport, we investigated GLUT4 translocation in C2C12-GLUT4myc myotubes. There was no effect of the Rac1 inhibitor NSC23766 on AICAR or DNP-induced GLUT4 translocation (Fig. 7*G*), which is in accordance with our observation that Rac1 is not activated in response to these stimuli in C2C12-GLUT4myc myotubes.

Contraction-stimulated 2DG uptake is inhibited by actin cytoskeleton depolymerization. Rac1 is a major regulator of actin remodeling, and cytoskeletal rearrangement is required for GLUT4 translocation in response to insulin (17,37). Because we found that inhibition of Rac1 decreased contraction-stimulated glucose uptake, we hypothesized that this might be due to impaired Rac1-dependent regulation of the actin cytoskeleton. At concentrations that have previously been found to inhibit insulin-stimulated glucose uptake in rat skeletal muscle (38), the actin depolymerizing agent, Latrunculin B, blocked contraction-induced 2DG uptake in soleus and decreased 2DG uptake by 62% in EDL muscle (Fig. 8*A*). However, this concentration inhibited initial force production by ~50% (Supplementary Fig. 1*C*). Therefore, soleus and EDL muscles were also incubated with one-tenth of the previously applied concentration. This concentration did not inhibit force production (Supplementary Fig. 1*C*) (and hence is deemed unlikely to affect contractile actin filaments), yet inhibited contraction-stimulated glucose uptake in soleus by 25% and EDL by ~40% (Fig. 8*B*). These results suggest that an intact actin cytoskeleton is necessary for muscle contraction to stimulate glucose uptake in skeletal muscle.

DISCUSSION

This study demonstrates that Rac1 and its downstream target, PAK1, are activated by exercise in human and mouse skeletal muscles. We further show, using an AMPK α2-KD mouse model, that activation of Rac1 during treadmill running does not depend on α2-AMPK, and that AMPK-activating agents, such as AICAR and DNP, do not activate Rac1 in intact muscle or muscle cell culture. Finally, using pharmacological inhibitors as well as inducible, muscle-specific Rac1 KO mice, Rac1 is identified as a novel regulator of contraction-induced but not AICAR-induced glucose uptake. Because Rac1 is activated by insulin in muscle (17,22), these findings indicate that Rac1 is a novel convergence point between insulin- and contraction-stimulated signaling pathways.

AMPK-independent Rac1 activation is inconsistent with a previous study, proposing a correlation between AMPK phosphorylation and Rac1-activity in response to AICAR and retinoic acid in muscle cells (19). However, that study used the unspecific AMPK inhibitor compound C, and although small interfering RNA toward AMPKα1 inhibited downstream targets of Rac1, the authors did not report inhibition of Rac1-GTP binding. We argue that AMPK-independent pathways mediate contraction-stimulated activation of Rac1 in skeletal muscle. Load-sensitive pathways were previously found to activate upstream effectors of Rac1 in vitro (39). Such pathways could therefore be activating Rac1 during muscle contraction because stretching activated Rac1 in the current study. Interestingly, we observed a relocation at the cell periphery of Rac1 in exercise-stimulated single muscle fibers. These data suggest that Rac1 is dynamically affected by exercise.

To elucidate the functional significance of Rac1 activation during exercise, the effect of two specific inhibitors of Rac1 was assessed, and both decreased contraction-stimulated glucose uptake in soleus and EDL muscles. Using a genetic Rac1 KO model, we further show that contraction-induced glucose uptake is lower in EDL muscles in which Rac1 content was only 10% of that in WT mice. In contrast, Rac1 KO only resulted in a tendency to decreased glucose uptake during muscle contractions in soleus muscle. We speculate that the remaining Rac1 content in soleus (35%) may have been sufficient to stimulate glucose uptake. The chemical inhibitors of Rac1 were more potent in reducing contraction-stimulated glucose uptake than the genetic model. This is potentially due to a more complete Rac1 inhibition or to nonspecific effects such as binding of the inhibitors to GLUT4 or interfering with other signals. However, in adipose tissue, which relies on the GTPase TC10 rather than Rac1 to regulate insulin-stimulated glucose uptake (16,40), Rac1 Inhibitor II did not inhibit insulin-stimulated glucose uptake. Also, AICAR-stimulated glucose transport was not affected by Rac1 Inhibitor II or Rac1 KO; in addition, AICAR and DNP-stimulated GLUT4 translocation was not inhibited by the Rac1 inhibitor NSC23766 in C2C12-GLUT4myc myotubes. We further demonstrated that these inhibitors did not affect AMPK and ACC phosphorylation or GLUT4 and Rac1 protein expression. This suggests that the inhibitors did not directly affect the GLUT4 translocation machinery and shows that Rac1 is involved in contraction-stimulated but not AICAR- or DNP-stimulated glucose transport in skeletal muscle.

Previous studies have shown that contraction-stimulated glucose uptake directly correlates with force development in incubated muscles (41). However, the Rac1 inhibitors in the current study did not decrease tension development during contractions. The intracellular potency of the inhibitor was further verified by measuring the phosphorylation status of PAK1, the Rac1 downstream target. Rac1 Inhibitor II more potently affected p-PAK^{Thr423} than was observed in the Rac1 KO model. Also, the elevated level of PAK1 protein in the Rac1 KO mice might have compensated for the lack of Rac1 in order to activate downstream signaling. It is therefore likely that the greater effect on glucose uptake observed in the inhibitor experiments compared with the experiments using the Rac1 KO model is because Rac1-signaling was more potently prevented by the inhibitor than by inducible Rac1 KO.

Despite complete blockade of Rac1 signaling (e.g., p-PAK^{Thr423}), we only observed ~55% reduction in contraction-stimulated glucose uptake with the inhibitors or Rac1 knockdown. Interestingly there seems to be fiber type-specific activation pattern for Rac1, because no

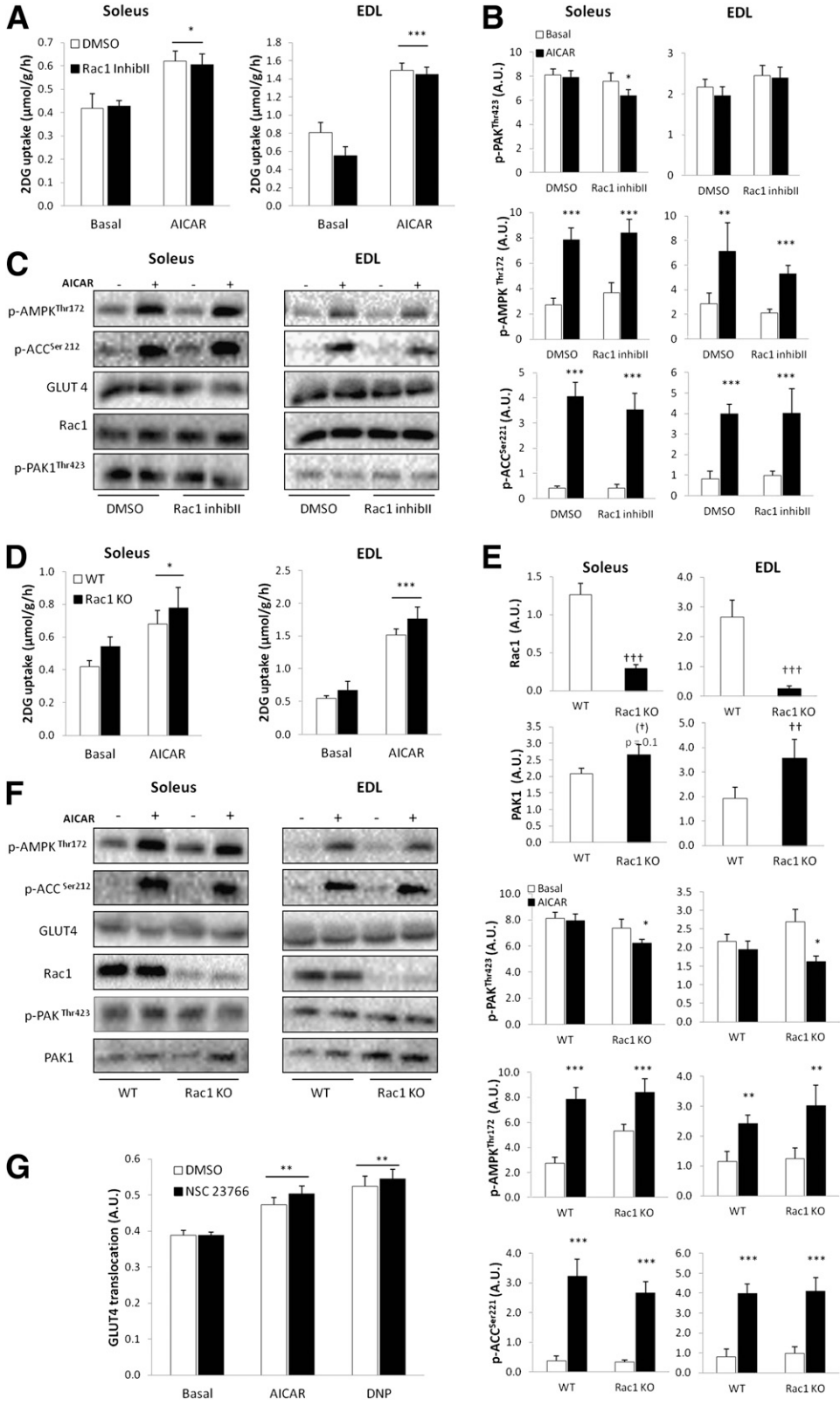

FIG. 7. ***A*: AICAR-stimulated (2 mmol/L) 2DG uptake in incubated isolated soleus and EDL without or with 10 µmol/L Rac1 Inhibitor II (Inhib II), 1-h preincubation (n = 8). *B*: Bar graphs show mean ± SEM of AICAR-induced p-AMPK ^{Thr172}, p-ACC ^{Ser212}, p-PAK^{Thr423}, in soleus and EDL without or with 10 µmol/L Rac1 Inhibitor II (Inhib II) (n = 8). *C*: Representative Western blots of p-AMPK^{Thr172}, p-ACC^{Ser212}, p-PAK^{Thr423}, and GLUT4 and Rac1 total proteins in response to AICAR without or with 10 µmol/L Rac1 Inhibitor II (Inhib II). *D*: AICAR-stimulated 2DG uptake in mouse soleus and EDL muscles from WT and muscle-specific inducible Rac1 KO (n = 8) mice. *E*: Bar graphs show mean ± SEM of AICAR-induced p-AMPK ^{Thr172}, p-ACC ^{Ser212}, p-PAK^{Thr423}, and total Rac1 and PAK1 protein in soleus and EDL muscles from WT or Rac1 KO mice (n = 8). *F*: Representative Western blots of p-AMPK^{Thr172}, p-ACC^{Ser212}, and p-PAK^{Thr423}/PAK1, and GLUT4, Rac1, and PAK1 total proteins in response to AICAR in WT and Rac1 KO soleus and EDL muscles. *G*: AICAR-stimulated GLUT4 translocation in C2C12-GLUT4myc myotubes in response to DNP (0.5 mmol/L) or AICAR (2 mmol/L) without or with 200 µmol/L NSC23766, 1-h preincubation (n = 6). Statistical significances between basal and AICAR are indicated by *P < 0.05; **P < 0.01; ***P < 0.001. Significant differences in AICAR-stimulated signaling are indicated by #P < 0.05. Main effect of genotype is indicated by ††P < 0.01 and †††P <0.0001. Values represent mean ± SEM.**

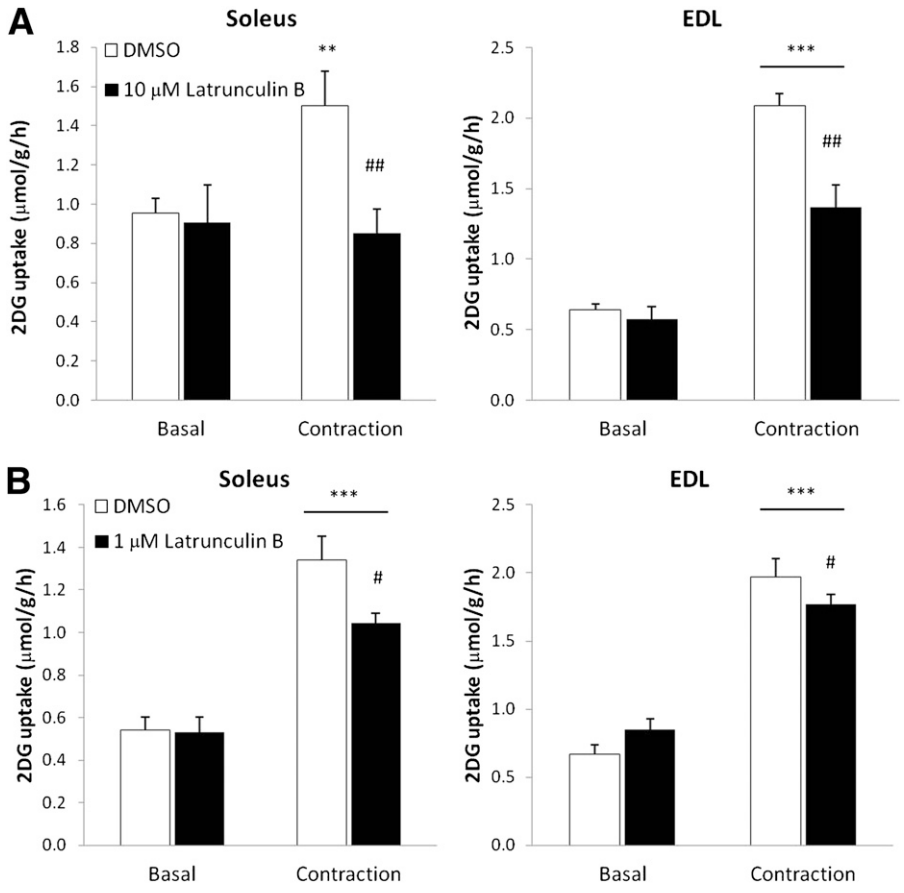

FIG. 8. ***A*: Contraction-stimulated 2DG uptake in mouse soleus and EDL without or with 10 μmol/L Latrunculin B, 1-h preincubation (n = 13–18). *B*: Contraction-stimulated 2DG uptake in mouse soleus and EDL without or with 1 μmol/L Latrunculin B, 1-h preincubation (n = 6–12). Statistical significances between basal and contraction are indicated by **$P < 0.01$; *** $P < 0.001$. Significant differences in contraction-stimulated glucose uptake are indicated by #$P < 0.05$; ## $P < 0.01$. Values represent mean ± SEM.**

increase in p-PAK^{Thr423} phosphorylation was observed in soleus muscle in response to contraction, despite the observation that Rac1-GTP binding increased. It is therefore possible that basal Rac1 activity may provide a permissive signal in order for contraction to induce glucose uptake.

AMPK-independent mechanisms regulating contraction-stimulated glucose uptake is in agreement with the literature, because studies investigating the involvement of AMPK show inconsistent results. In vitro, β1β2 AMPK KO or overexpression of the dominant negative α2 AMPK construct impairs (but does not prevent) contraction-induced glucose uptake (26,42), whereas no impairment was reported in another mouse model carrying inactive AMPK catalytic subunits (43). The role of AMPK in regulating contraction-stimulated glucose uptake is thus not clear, and other proteins might play major roles in this process. Calcium-dependent signals have also been known to participate in contraction-stimulated glucose uptake. Indeed, inhibition of CaMKII signaling decreases contraction-stimulated glucose uptake (44), unlike KO of PKC-α, one of the major proteins activated by calcium (45). Finally, nitric oxide and reactive oxygen species contributed to contraction-stimulated glucose uptake in some (46,47) but not other studies (48). Rac1 may be a novel candidate to add to our understanding of this complex signaling network.

Our study represents a first step in identifying Rac1 as a viable signal in the pathway of contraction-regulated glucose uptake. Unraveling the downstream signaling involved should be pursued next. This is unlikely to involve the AMPK pathway because the dampened contraction-stimulated glucose uptake of Rac1 KO muscles was not accompanied by changes in p-AMPK^{Thr172} or p-ACC^{Ser212}. Similarly, it is unlikely to involve Akt signaling because AS160/TBC1D4 phosphorylation assessed with a PAS antibody was not decreased in the KO muscles. In addition, when site-specific phosphorylation on TBC1D1^{Ser237} in EDL and TBC1D4^{Thr642} in soleus was measured, no difference between WT and KO was found. However, Rac1 KO mice had lower p-PAK^{Thr423}, and PAK1 has recently been implicated in insulin-stimulated GLUT4 translocation in skeletal muscle (49). Collectively, these arguments suggest the operation of distinct signaling pathways downstream of Rac1 toward glucose uptake.

Rac1 activation is necessary to induce actin remodeling in response to insulin, a process that leads to tethering, docking, and/or fusion of GLUT4 vesicles with the plasma membrane (16,17,37). In the current study, the actin-depolymerizing agent Latrunculin B reduced contraction-stimulated glucose uptake. It is therefore plausible that muscle contraction, like insulin, also relies on reorganization of the nonsarcomeric actin cytoskeleton to induce GLUT4 translocation and glucose uptake.

To our knowledge, the findings presented here are the first to indicate that Rac1 is involved in regulating contraction-stimulated glucose uptake. Further studies will be required to establish whether the cytoskeleton

(irrespective of the contractile machinery) or alternative mechanisms underlie this novel input of Rac1 in the regulation of contraction-induced glucose uptake.

ACKNOWLEDGMENTS

The study was supported by grants from the Danish Diabetes Association, the Danish Medical Research Council, the Novo Nordisk Foundation, The Lundbeck Foundation, the Universitetsforskningens Investerings Kapital–Food Fitness and Pharma, and Grant MT-12601 from Canadian Institutes of Health Research to A.K.

S.J.M. is employed by Novo Nordisk A/S, Søborg, Denmark. No other potential conflicts of interest relevant to this article were reported.

L.S. designed the study, conducted the experiments, performed the laboratory analysis, and wrote and commented on the manuscript. T.E.J. designed the study, took part in conducting the experiments and laboratory analysis, and commented on the manuscript. M.K., S.J.M., J.J., and C.P. took part in conducting the experiments and commented on the manuscript. J.R.M., T.T.C., and S.B. took part in conducting the experiments. A.K. provided the C2C12 myotubes and commented on the manuscript. P.S. and E.A.R. designed the study and commented on the manuscript. E.A.R. is the guarantor of this work and, as such, had full access to all the data in the study and takes responsibility for the integrity of the data and the accuracy of the data analysis.

The authors acknowledge the skilled technical assistance of Betina Bolmgren (Molecular Physiology Group, Denmark). AMPK KD founder mice were a kind gift from Morris J. Birnbaum (Pennsylvania School of Medicine, U.S.). Rac1 floxed founder mice were a kind gift from Cord Brakebusch (Biomedical Institute, BRIC, University of Copenhagen, Denmark). Tetracycline-activated Cre founder mice were a kind gift from Ashley Monks (Department of Psychology, University of Toronto Mississauga, Mississauga, Ontario, Canada). Microscopy was performed at the Core Facility for Integrated Microscopy (www.cfim.ku.dk).

REFERENCES

1. Goldstein MS, Mullick V, Huddlestun B, Levine R. Action of muscular work on transfer of sugars across cell barriers; comparison with action of insulin. Am J Physiol 1953;173:212–216
2. Holloszy JO, Narahara HT. Studies of tissue permeability. X. Changes in permeability to 3-methylglucose associated with contraction of isolated frog muscle. J Biol Chem 1965;240:3493–3500
3. Rose AJ, Richter EA. Skeletal muscle glucose uptake during exercise: how is it regulated? Physiology (Bethesda) 2005;20:260–270
4. Lauritzen HP, Reynet C, Schjerling P, et al. Gene gun bombardment-mediated expression and translocation of EGFP-tagged GLUT4 in skeletal muscle fibres in vivo. Pflugers Arch 2002;444:710–721
5. Klip A, Ramlal T, Young DA, Holloszy JO. Insulin-induced translocation of glucose transporters in rat hindlimb muscles. FEBS Lett 1987;224:224–230
6. Treadway JL, James DE, Burcel E, Ruderman NB. Effect of exercise on insulin receptor binding and kinase activity in skeletal muscle. Am J Physiol 1989;256:E138–E144
7. Goodyear LJ, Giorgino F, Balon TW, Condorelli G, Smith RJ. Effects of contractile activity on tyrosine phosphoproteins and PI 3-kinase activity in rat skeletal muscle. Am J Physiol 1995;268:E987–E995
8. Wojtaszewski JF, Higaki Y, Hirshman MF, et al. Exercise modulates postreceptor insulin signaling and glucose transport in muscle-specific insulin receptor knockout mice. J Clin Invest 1999;104:1257–1264
9. Lee AD, Hansen PA, Holloszy JO. Wortmannin inhibits insulin-stimulated but not contraction-stimulated glucose transport activity in skeletal muscle. FEBS Lett 1995;361:51–54
10. Richter EA, Garetto LP, Goodman MN, Ruderman NB. Muscle glucose metabolism following exercise in the rat: increased sensitivity to insulin. J Clin Invest 1982;69:785–793
11. Maarbjerg SJ, Sylow L, Richter EA. Current understanding of increased insulin sensitivity after exercise - emerging candidates. Acta Physiol (Oxf) 2011;202:323–335
12. Winder WW, Hardie DG. Inactivation of acetyl-CoA carboxylase and activation of AMP-activated protein kinase in muscle during exercise. Am J Physiol 1996;270:E299–E304
13. Jessen N, Goodyear LJ. Contraction signaling to glucose transport in skeletal muscle. J Appl Physiol 2005;99:330–337
14. Chiu TT, Jensen TE, Sylow L, Richter EA, Klip A. Rac1 signalling towards GLUT4/glucose uptake in skeletal muscle. Cell Signal 2011;23:1546–1554
15. Hall A, Nobes CD. Rho GTPases: molecular switches that control the organization and dynamics of the actin cytoskeleton. Philos Trans R Soc Lond B Biol Sci 2000;355:965–970
16. JeBailey L, Rudich A, Huang X, Di Ciano-Oliveira C, Kapus A, Klip A. Skeletal muscle cells and adipocytes differ in their reliance on TC10 and Rac for insulin-induced actin remodeling. Mol Endocrinol 2004;18:359–372
17. JeBailey L, Wanono O, Niu W, Roessler J, Rudich A, Klip A. Ceramide- and oxidant-induced insulin resistance involve loss of insulin-dependent Rac-activation and actin remodeling in muscle cells. Diabetes 2007;56:394–403
18. Ueda S, Kataoka T, Satoh T. Activation of the small GTPase Rac1 by a specific guanine-nucleotide-exchange factor suffices to induce glucose uptake into skeletal-muscle cells. Biol Cell 2008;100:645–657
19. Lee YM, Lee JO, Jung JH, et al. Retinoic acid leads to cytoskeletal rearrangement through AMPK-Rac1 and stimulates glucose uptake through AMPK-p38 MAPK in skeletal muscle cells. J Biol Chem 2008;283:33969–33974
20. Kou R, Sartoretto J, Michel T. Regulation of Rac1 by simvastatin in endothelial cells: differential roles of AMP-activated protein kinase and calmodulin-dependent kinase kinase-beta. J Biol Chem 2009;284:14734–14743
21. Bae HB, Zmijewski JW, Deshane JS, et al. AMP-activated protein kinase enhances the phagocytic ability of macrophages and neutrophils. FASEB J 2011;25:4358–4368
22. Ueda S, Kitazawa S, Ishida K, et al. Crucial role of the small GTPase Rac1 in insulin-stimulated translocation of glucose transporter 4 to the mouse skeletal muscle sarcolemma. FASEB J 2010;24:2254–2261
23. Mu J, Brozinick JT Jr, Valladares O, Bucan M, Birnbaum MJ. A role for AMP-activated protein kinase in contraction- and hypoxia-regulated glucose transport in skeletal muscle. Mol Cell 2001;7:1085–1094
24. Chrostek A, Wu X, Quondamatteo F, et al. Rac1 is crucial for hair follicle integrity but is not essential for maintenance of the epidermis. Mol Cell Biol 2006;26:6957–6970
25. Rao P, Monks DA. A tetracycline-inducible and skeletal muscle-specific Cre recombinase transgenic mouse. Dev Neurobiol 2009;69:401–406
26. Jensen TE, Rose AJ, Jørgensen SB, et al. Possible CaMKK-dependent regulation of AMPK phosphorylation and glucose uptake at the onset of mild tetanic skeletal muscle contraction. Am J Physiol Endocrinol Metab 2007;292:E1308–E1317
27. Maarbjerg SJ, Jørgensen SB, Rose AJ, et al. Genetic impairment of AMPKalpha2 signaling does not reduce muscle glucose uptake during treadmill exercise in mice. Am J Physiol Endocrinol Metab 2009;297:E924–E934
28. Jeppesen J, Albers PH, Rose AJ, et al. Contraction-induced skeletal muscle FAT/CD36 trafficking and FA uptake is AMPK independent. J Lipid Res 2011;52:699–711
29. Zhou M, Sevilla L, Vallega G, et al. Insulin-dependent protein trafficking in skeletal muscle cells. Am J Physiol 1998;275:E187–E196
30. Niu W, Bilan PJ, Ishikura S, et al. Contraction-related stimuli regulate GLUT4 traffic in C2C12-GLUT4myc skeletal muscle cells. Am J Physiol Endocrinol Metab 2010;298:E1058–E1071
31. Jensen TE, Leutert R, Rasmussen ST, et al. EMG-normalised kinase activation during exercise is higher in human gastrocnemius compared to soleus muscle. PLoS ONE 2012;7:e31054
32. Ploug T, van Deurs B, Ai H, Cushman SW, Ralston E. Analysis of GLUT4 distribution in whole skeletal muscle fibers: identification of distinct storage compartments that are recruited by insulin and muscle contractions. J Cell Biol 1998;142:1429–1446
33. Castro-Castro A, Ojeda V, Barreira M, et al. Coronin 1A promotes a cytoskeletal-based feedback loop that facilitates Rac1 translocation and activation. EMBO J 2011;30:3913–3927
34. Navarro-Lerida I, Sanchez-Perales S, Calvo M, et al. A palmitoylation switch mechanism regulates Rac1 function and membrane organization. EMBO J 2011;31:534–551
35. Rose AJ, Jeppesen J, Kiens B, Richter EA. Effects of contraction on localization of GLUT4 and v-SNARE isoforms in rat skeletal muscle. Am J Physiol Regul Integr Comp Physiol 2009;297:R1228–R1237

36. Schoentaube J, Olling A, Tatge H, Just I, Gerhard R. Serine-71 phosphorylation of Rac1/Cdc42 diminishes the pathogenic effect of Clostridium difficile toxin A. Cell Microbiol 2009;11:1816–1826
37. Török D, Patel N, Jebailey L, et al. Insulin but not PDGF relies on actin remodeling and on VAMP2 for GLUT4 translocation in myoblasts. J Cell Sci 2004;117:5447–5455
38. Brozinick JT Jr, Hawkins ED, Strawbridge AB, Elmendorf JS. Disruption of cortical actin in skeletal muscle demonstrates an essential role of the cytoskeleton in glucose transporter 4 translocation in insulin-sensitive tissues. J Biol Chem 2004;279:40699–40706
39. Zhou Y, Jiang D, Thomason DB, Jarrett HW. Laminin-induced activation of Rac1 and JNKp46 is initiated by Src family kinases and mimics the effects of skeletal muscle contraction. Biochemistry 2007;46:14907–14916
40. Chiang SH, Baumann CA, Kanzaki M, et al. Insulin-stimulated GLUT4 translocation requires the CAP-dependent activation of TC10. Nature 2001; 410:944–948
41. Ihlemann J, Ploug T, Hellsten Y, Galbo H. Effect of tension on contraction-induced glucose transport in rat skeletal muscle. Am J Physiol 1999;277: E208–E214
42. O'Neill HM, Maarbjerg SJ, Crane JD, et al. AMP-activated protein kinase (AMPK) beta1beta2 muscle null mice reveal an essential role for AMPK in maintaining mitochondrial content and glucose uptake during exercise. Proc Natl Acad Sci U S A 2011;108:16092–16097
43. Fujii N, Hirshman MF, Kane EM, et al. AMP-activated protein kinase alpha2 activity is not essential for contraction- and hyperosmolarity-induced glucose transport in skeletal muscle. J Biol Chem 2005;280:39033–39041
44. Witczak CA, Jessen N, Warro DM, et al. CaMKII regulates contraction- but not insulin-induced glucose uptake in mouse skeletal muscle. Am J Physiol Endocrinol Metab 2010;298:E1150–E1160
45. Jensen TE, Maarbjerg SJ, Rose AJ, Leitges M, Richter EA. Knockout of the predominant conventional PKC isoform, PKCalpha, in mouse skeletal muscle does not affect contraction-stimulated glucose uptake. Am J Physiol Endocrinol Metab 2009;297:E340–E348
46. Sandström ME, Zhang SJ, Bruton J, et al. Role of reactive oxygen species in contraction-mediated glucose transport in mouse skeletal muscle. J Physiol 2006;575:251–262
47. Merry TL, Lynch GS, McConell GK. Downstream mechanisms of nitric oxide-mediated skeletal muscle glucose uptake during contraction. Am J Physiol Regul Integr Comp Physiol 2010;299:R1656–R1665
48. Rottman JN, Bracy D, Malabanan C, Yue Z, Clanton J, Wasserman DH. Contrasting effects of exercise and NOS inhibition on tissue-specific fatty acid and glucose uptake in mice. Am J Physiol Endocrinol Metab 2002;283: E116–E123
49. Wang Z, Oh E, Clapp DW, Chernoff J, Thurmond DC. Inhibition or ablation of p21-activated kinase (PAK1) disrupts glucose homeostatic mechanisms in vivo. J Biol Chem 2011;286:41359–41367